

Structure-aware divergences for comparing probability distributions

Rohit Sahasrabudde ^{1,2,*} and Renaud Lambiotte ^{1,3}

¹*Mathematical Institute, University of Oxford, Oxford, United Kingdom*

²*Institute for New Economic Thinking, University of Oxford, Oxford, United Kingdom*

³*Complexity Science Hub, Vienna, Austria*

(Dated: March 24, 2026)

Many natural and social science systems are described using probability distributions over elements that are related to each other: for instance, occupations with shared skills or species with similar traits. Standard information theory quantities such as entropies and f -divergences treat elements interchangeably and are blind to the similarity structure. We introduce a family of divergences that are sensitive to the geometry of the underlying domain. By virtue of being the Bregman divergences of structure-aware entropies, they provide a framework that retains several advantages of Kullback-Leibler divergence and Shannon entropy. Structure-aware divergences recover planted patterns in a synthetic clustering task that conventional divergences miss and are orders of magnitude faster than optimal transport distances. We demonstrate their applicability in economic geography and ecology, where structure plays an important role. Modelling different notions of occupation relatedness yields qualitatively different regionalisations of their geographic distribution. Our methods also reproduce established insights into functional β -diversity in ecology obtained with optimal transport methods.

I. INTRODUCTION

In many natural and social systems, probability distributions are defined over elements that are related to each other. Evidence from a variety of disciplines shows that this structure contains crucial information that cannot be discarded. Many researchers have advocated against the dichotomy of elements being identical or completely distinct. For instance, in evolutionary economic geography, the principle of relatedness posits that economic agents tend to expand their capability base by acquiring new capabilities that are similar to their existing ones. Relatedness is used to explain phenomena across scales: from the export baskets of countries [1], to how industries enter and exit regions [2, 3], and the productivity and diversification of cities [4, 5]. For a recent review, see Hidalgo et al. [6].

In ecology, measuring the diversity of an ecosystem from its species composition is a long-studied task [7]. Ecologists have devised many structure-aware indices to capture the intuition that populations with dissimilar species are more diverse. For recent surveys of the mathematics of diversity indices, see Daly et al. [8] and Leinster [9]. Species similarity is particularly important in functional ecology, which focuses on the functional role of species in the ecosystem rather than their taxonomic classification [10, 11]. Functions are often proxied by traits [12] and species with similar traits are considered to play similar roles in the community [13].

Our work is motivated by information theory [14], which provides a suite of tools to analyse distributions. Consider the tasks of measuring (i) the spread of a distribution and (ii) the dissimilarity of a pair of distributions. Quantities such as Shannon entropy [15] and

its generalisations [16, 17] have been used to measure spread in a variety of disciplines, including economic geography [2] and ecology [18, 19]. Distance-like functions such as Kullback-Leibler (KL) divergence [20] and other f -divergences [16, 21] are common ways to compare distributions. Entropies and divergences have a convenient geometry when used together as a toolkit for analysing distributions [14, 22]. However, they are blind to the similarity structure of their domains.

There are many approaches to incorporate similarity into entropy or diversity measures, from Rao's foundational work [23] and its application to graphs [24] to Leinster and Cobbold's [25] recent contributions. However, we lack corresponding divergences that can be used to compare distributions. In this article, we fill this gap by introducing a novel family of structure-aware divergences. Building on KL divergence's geometric connection with Shannon entropy, we construct them from Ricotta and Szeidl's structure-aware entropies [26].

The comparison of distributions over sets with structure dates back to Monge [27], whose work in the 1700s is the root of Optimal Transport (OT) theory [28]. OT measures the minimum cost of transforming one distribution into another, where costs are defined using the underlying metric space. Computing OT distances such as the Wasserstein metric [29, 30] involves solving a costly optimisation problem. In contrast, our family of divergences has a closed form expression, which allows efficient computation and analytical study. By virtue of being Bregman divergences [31], they have several convenient properties [22, 32] that make them suitable for clustering [32] and projections [33].

In a synthetic clustering experiment, we show that structure-aware divergence recovers planted patterns that are lost when structure is discarded. In a separate numerical experiment, we demonstrate that it is substantially faster to compute than the Wasserstein distance.

* Corresponding author: rohit.sahasrabudde@maths.ox.ac.uk

Applied to the geographic distribution of occupations in England and Wales, structure-aware methods reveal how different definitions of relatedness lead to distinct regionalisations. Analysing data from vegetation in the Rutor glacier, we reproduce insights on β -diversity previously established with OT methods.

II. RESULTS

A. Preliminaries

Through this article, we denote vectors and matrices in bold and their entries in regular font. For instance, p_i is the i^{th} entry of vector \mathbf{p} . $\mathbf{1}$ represents the vector of ones and \mathbf{I} the identity matrix. Their dimension will be clear in context. We often employ vector notation to avoid clunky summations. We will use n and m for integers.

Let \mathcal{X} be a finite set with $n \geq 1$ elements. We represent a probability distribution over \mathcal{X} as a vector \mathbf{p} .

Definition 1. The **probability simplex** $\Delta_n \subset \mathbb{R}^n$ contains all the probability distributions over n elements.

$$\Delta_n = \{\mathbf{p} \in \mathbb{R}^n \mid \mathbf{1}^\top \mathbf{p} = 1, \mathbf{p} \geq 0\} \quad (1)$$

Δ_n° is its relative interior, containing all the distributions of full support.

$$\Delta_n^\circ = \{\mathbf{p} \in \Delta_n \mid \mathbf{p} > 0\} \quad (2)$$

We write the pairwise similarities between the elements of \mathcal{X} in a matrix \mathbf{Z} . Our methods are agnostic of how similarity is defined, as long as it has the following properties.

Definition 2. A matrix $\mathbf{Z} \in \mathbb{R}^{n \times n}$ is a **similarity matrix** if $0 \leq \mathbf{Z} \leq \mathbf{1}$, $\mathbf{Z}^\top = \mathbf{Z}$, and $Z_{ii} = 1$.

Similarity is positive, symmetric, and bounded. Each element is maximally similar to itself. The case of unrelated elements corresponds to $\mathbf{Z} = \mathbf{I}$.

B. Structure-aware entropy

How do we measure the spread of a distribution \mathbf{p} ? Intuitively, a distribution is more spread out if high probability elements are dissimilar. The Simpson concentration [34] of \mathbf{p} is the probability that two elements chosen independently at random according to \mathbf{p} are identical. The same quantity is known as the Herfindahl–Hirschman index in economics. A natural structure-aware generalisation of this idea is the expected dissimilarity of two elements, proposed by Rao [23]. Ricotta and Szeidl [26] generalised this further by incorporating structure into the Havrda-Charvát (HC) entropies [17].

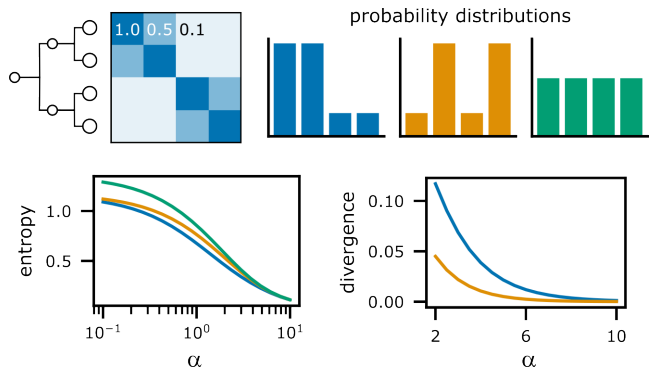


FIG. 1. **Illustrative example.** \mathbf{Z} is a similarity matrix representing a two-level hierarchy where four elements group into ‘pairs’ (top left). We consider three distributions over them: one where both elements of a pair have high probability (blue), one where one element each from the pairs have high probability (orange), and the uniform distribution (green; top right). The orange distribution has a higher entropy than the blue one since its high probability elements are dissimilar (bottom left; note the log scale for α). Similarly, the orange distribution diverges less from the uniform distribution than the blue one does (bottom right; note that divergence is only defined for $\alpha \geq 2$). Entropies and divergences blind to structure would not differentiate between the two.

Definition 3. The **structure-aware HC entropy** of order $\alpha \in [0, \infty)$ of $\mathbf{p} \in \Delta_n$ is

$$\mathcal{H}_\alpha^{\mathbf{Z}}(\mathbf{p}) = \frac{1}{\alpha - 1} (1 - \mathbf{p}^\top (\mathbf{Z}\mathbf{p})^{\alpha-1}), \quad (3)$$

for $\alpha \neq 1$, and

$$\mathcal{H}_1^{\mathbf{Z}}(\mathbf{p}) = -\mathbf{p}^\top \ln(\mathbf{Z}\mathbf{p}), \quad (4)$$

where $0 \ln 0 := 0$ and the powers and logarithm are element-wise.

$\mathcal{H}_2^{\mathbf{Z}}$ is Rao’s index and we recover the original HC entropies by setting $\mathbf{Z} = \mathbf{I}$, including the Gini-Simpson index for $\alpha = 2$ and Shannon entropy for $\alpha = 1$. In Fig. 1, the blue and orange distributions have identical entropy without structure, while $\mathcal{H}_\alpha^{\mathbf{Z}}$ is higher for the orange one since it assigns high probability to dissimilar elements.

In information theoretic fashion, structure-aware entropy can be interpreted in terms of surprise [25]. The ‘ordinariness’ of i is $(\mathbf{Z}\mathbf{p})_i = \sum_j Z_{ij} p_j \in [0, 1]$ – its expected similarity to an element picked at random according to \mathbf{p} . An element is ordinary if it is abundant or similar to abundant elements. The surprise of an element is a decreasing function of its ordinariness. When this function is

$$x \mapsto \begin{cases} \frac{1}{\alpha-1} (1 - x^{\alpha-1}) & \text{for } \alpha \neq 1, \\ -\ln x & \text{for } \alpha = 1, \end{cases} \quad (5)$$

$\mathcal{H}_\alpha^{\mathbf{Z}}$ is the expected surprise. Increasing α decreases surprise, affecting the less ordinary elements more (see

Methods). Thus, α can be used to tune the sensitivity of $\mathcal{H}_\alpha^{\mathbf{Z}}$ to rare elements.

Leinster and Cobbold [25] generalised other measures such as the Rényi entropies [16] and Hill numbers [18] to be structure-aware. However, even in the structure-blind case, only the HC entropies are concave. We will see that this is crucial to our methods.

C. Structure-aware divergence

How do we compare two distributions? To formulate a structure-aware analogue of KL divergence [20], we turn to its geometric connection with Shannon entropy: it is the Bregman divergence [31] induced by negative entropy.

Definition 4. Let $\Omega \subseteq \mathbb{R}^n$ be a convex set and $\phi : \Omega \rightarrow \mathbb{R}$ a strictly convex function that is differentiable in its relative interior $\text{ri}(\Omega)$. The associated **Bregman divergence** $d_\phi : \Omega \times \text{ri}(\Omega) \rightarrow [0, \infty)$ is

$$d_\phi(\omega_1 \parallel \omega_2) = \phi(\omega_1) - \phi(\omega_2) - \langle \nabla \phi(\omega_2), \omega_1 - \omega_2 \rangle. \quad (6)$$

The divergence of ω_1 from ω_2 is the difference between $\phi(\omega_1)$ and its first-order approximation from ω_2 . Many other distance-like functions such as squared Mahalanobis distance, Itakura-Saito distance, and logistic loss are also Bregman divergences [32, Table 1] and they have several convenient properties [32, Appendix A].

This machinery provides a way to construct a divergence from an entropy. However, it requires convexity and unlike negative Shannon entropy, $-\mathcal{H}_\alpha^{\mathbf{Z}}$ is not strictly convex in general. Building on Ricotta and Szeidl [26], we identify sufficient conditions.

Theorem 1. $\mathcal{H}_\alpha^{\mathbf{Z}}$ is strictly concave in Δ_n° for $\alpha \geq 2$ if $\mathbf{Z} \succ 0$.

Note that our result is for the interior of the simplex (see Methods for proof). This is not particularly restrictive and we ensure it in practice by setting zero entries to a small positive constant. When the conditions are met and entropy is strictly concave, negative entropy is strictly convex and we define its Bregman divergence as structure-aware divergence.

Definition 5. For $\alpha \geq 2$ and $\mathbf{Z} \succ 0$, the **structure-aware divergence** of order α is the function $d_\alpha^{\mathbf{Z}} : \Delta_n^\circ \times \Delta_n^\circ \rightarrow [0, \infty)$ defined as follows.

$$d_\alpha^{\mathbf{Z}}(\mathbf{p} \parallel \mathbf{q}) = \frac{1}{\alpha - 1} \mathbf{p}^\top \left((\mathbf{Z}\mathbf{p})^{\alpha-1} - (\mathbf{Z}\mathbf{q})^{\alpha-1} \right) - \mathbf{q}^\top \text{diag} \left((\mathbf{Z}\mathbf{q})^{\alpha-2} \right) \mathbf{Z}(\mathbf{p} - \mathbf{q}), \quad (7)$$

where the powers are element-wise.

Ignoring structure, the blue and orange distributions have the same divergence from the green one in Fig. 1.

However, in the blue distribution, the difference in probability from the green one is similar for similar elements. Structure-aware divergence captures the intuition that this makes it more dissimilar than the orange distribution. The divergence induced by Rao's index is the squared Mahalanobis distance [35]: $d_2^{\mathbf{Z}}(\mathbf{p} \parallel \mathbf{q}) = (\mathbf{p} - \mathbf{q})^\top \mathbf{Z}(\mathbf{p} - \mathbf{q})$. $d_\alpha^{\mathbf{Z}}(\mathbf{p} \parallel \mathbf{q}) \geq 0$, with equality if and only if $\mathbf{p} = \mathbf{q}$, it is convex in \mathbf{p} , and has the mean-minimiser property, which makes it particularly suited to clustering tasks (see Methods).

Note that formulating a clustering problem requires a way to measure how dispersed a set of distributions is. This is captured by Bregman information, which generalises variance and mutual information [32].

Definition 6. For $\alpha \geq 2$ and $\mathbf{Z} \succ 0$, consider $m \geq 1$ distributions $(\mathbf{p}^1, \dots, \mathbf{p}^m)$ with each $\mathbf{p}^a \in \Delta_n^\circ$. Let $\mathbf{w} \in \Delta_m$ be their weights. The **Bregman information** of this collection of distributions is

$$\begin{aligned} \mathbb{I}_\alpha^{\mathbf{Z}}((\mathbf{p}^a); \mathbf{w}) &= \sum_{a=1}^m w_a d_\alpha^{\mathbf{Z}}(\mathbf{p}^a \parallel \boldsymbol{\mu}) \\ &= \mathcal{H}_\alpha^{\mathbf{Z}}(\boldsymbol{\mu}) - \sum_{a=1}^m w_a \mathcal{H}_\alpha^{\mathbf{Z}}(\mathbf{p}^a), \end{aligned} \quad (8)$$

where $\boldsymbol{\mu} = \sum_a w_a \mathbf{p}^a \in \Delta_n^\circ$ is the mean.

$\mathbb{I}_\alpha^{\mathbf{Z}}$ is equivalently the expected divergence from the mean and the Jensen gap of negative entropy. This equivalence is implicit from the definition of the $d_\alpha^{\mathbf{Z}}$ (see Methods). For a partition, the total Bregman information can be written as a sum over between and within-cluster informations. The fraction that between-cluster accounts for measures how well the partition explains the data. Jensen-Bregman divergence is the Bregman information of two distributions and serves as a symmetric comparison.

D. Positive definite similarity matrices

How do we construct positive definite similarity matrices? The literature on metric spaces provides a remarkably powerful route. Let d be a metric on \mathcal{X} that creates a distance matrix \mathbf{D} . Defining $Z_{ij} = \exp(-\tau D_{ij})$ for some scaling constant $\tau > 0$ guarantees that \mathbf{Z} satisfies the range and symmetry conditions of similarity matrices. Meckes [36, Theorem 3.3] showed that $\mathbf{Z} \succ 0$ for all $\tau > 0$ if and only if d is a metric of negative type (see Methods). Many metric spaces that arise naturally in real systems satisfy this. For instance,

- subsets of Euclidean space (embeddings),
- any metric space with at most four points [36],
- weighted trees with the shortest path distance (hierarchies) [37], and
- undirected graphs with the effective resistance distance (diffusion on graphs) [38, 39].

If a similarity matrix defined in another way fails to be positive definite, we can attempt to find the best alternative. Finding the nearest positive definite similarity matrix can be framed as a convex optimisation problem (see Methods).

E. Synthetic experiments

1. Recovering planted partitions

Our first synthetic experiment shows that a clustering pipeline built on $d_\alpha^{\mathbf{Z}}$ recovers partitions planted in the similarity structure. The experiment is designed for simplicity, allowing us to illustrate the differences between the conventional (\mathbf{I}) and structure-aware (\mathbf{Z}) approaches.

Consider a set with 60 elements organised in three groups of 20 each. We embed elements in \mathbb{R}^2 , placing the groups cohesively (Fig. 2A, top). The triangle and square groups are closer to each other than they are to the circle. We construct a distribution by picking a group and sampling m elements from it with replacement. In a single run of the experiment, we generate ten distributions each from the three groups and cluster them (see Methods). We report results over 50 runs for each m .

Two distributions sampled from the same group may have no elements in common, making it impossible to distinguish between them and a pair from different groups without structural information. Distributions are less likely to overlap for low m . What effect does this have on the quality of partitions? The fraction of Bregman information explained by a partition measures its quality of fit [32]. The quality of the best partition always increases with the number of clusters k , with elbows suggesting optima (Fig. 2A, bottom left). While there is no clear elbow for \mathbf{I} when $m = 2$, we see one for \mathbf{Z} , indicating that incorporating structure enables us to identify the planted optimum k from under-sampled data.

Clustering quality only measures if the clusters explain the data. Do we recover the planted patterns? The ground truth for $k = 3$ is distributions being clustered by the group they were sampled from. We expect the triangle and square group to merge for $k = 2$. We recover the ground truth with \mathbf{Z} for both k perfectly for all m (Fig. 2A, bottom right). Without structure, we must rely on distributions overlapping to cluster them. For $k = 3$, we find the planted partition for high enough m . Since the distributions from triangles and squares never overlap by construction, it is impossible to find the two-cluster ground truth with \mathbf{I} . This simple experiment demonstrates how structure-blind methods can completely fail to provide insights into systems where structure is important.

2. Runtime compared to Optimal Transport

OT provides a suite of tools to compare distributions over metric spaces [28]. While computing the OT dissimilarity of two distributions involves solving an optimisation problem, our approach has closed-form expressions. Consider the problem of measuring the pairwise dissimilarity of distributions in a given set. Sampling these uniformly at random from Δ_n , we compare the runtime of the following approaches (see Methods for details).

- OT: Wasserstein-1 distance [29, 30] iterating over each pair.
- J-BD (naive): Jensen-Bregman divergence iterating over each pair.
- J-BD (fast): Jensen-Bregman divergence vectorised.

J-BD (naive) is roughly an order of magnitude faster than OT for all input sizes (Fig. 2B for $\alpha = 2$). J-BD (fast) is quicker still and scales better with input size. The results are qualitatively identical for $\alpha = 3$ (see SI Appendix). Unless the OT formulation is physically meaningful to the system, our approach is a faster alternative to make structure-aware comparisons. Note that they are fundamentally different ways of comparing distributions and might have different results. In this experiment, OT and J-BD dissimilarity have a Pearson’s $r \approx 0.92$ and Kendall’s $\tau \approx 0.77$ for all input sizes. These correlations may be sensitive to parameter choices.

F. The geography of occupations in England and Wales

A region’s occupational composition serves as a proxy for its capability base, which shapes key features such as resilience to shocks and the ability to diversify into new economic activities [3]. Daniotti et al. [5] found large-scale patterns in how the ‘coherence’ of cities varies with time and population size. They define coherence as the expected similarity of the occupations of two randomly sampled workers. In our framework, coherence is exactly $1 - \mathcal{H}_2^{\mathbf{Z}}$. This motivates using structure-aware divergence to compare the occupational compositions, and therefore the capability bases, of regions.

We analyse occupation data from the 2021 census of England and Wales at the geographic scale of Local Authorities (LAs). We proxy each LA’s capability base as its employment shares in occupations that produce tradable output, excluding occupations such as health service and retail workers that cater mainly to the local population [5]. We identify 41 such occupations and represent each of the 318 LAs as a distribution over them (see Methods).

There are several ways to conceptualise the relatedness of occupations. We construct similarity matrices for two commonly-used notions: occupations are related if (i) they require the same skills – skills similarity or (ii) the same regions specialise in them – co-location similarity (see Methods). Co-located occupations tend to belong

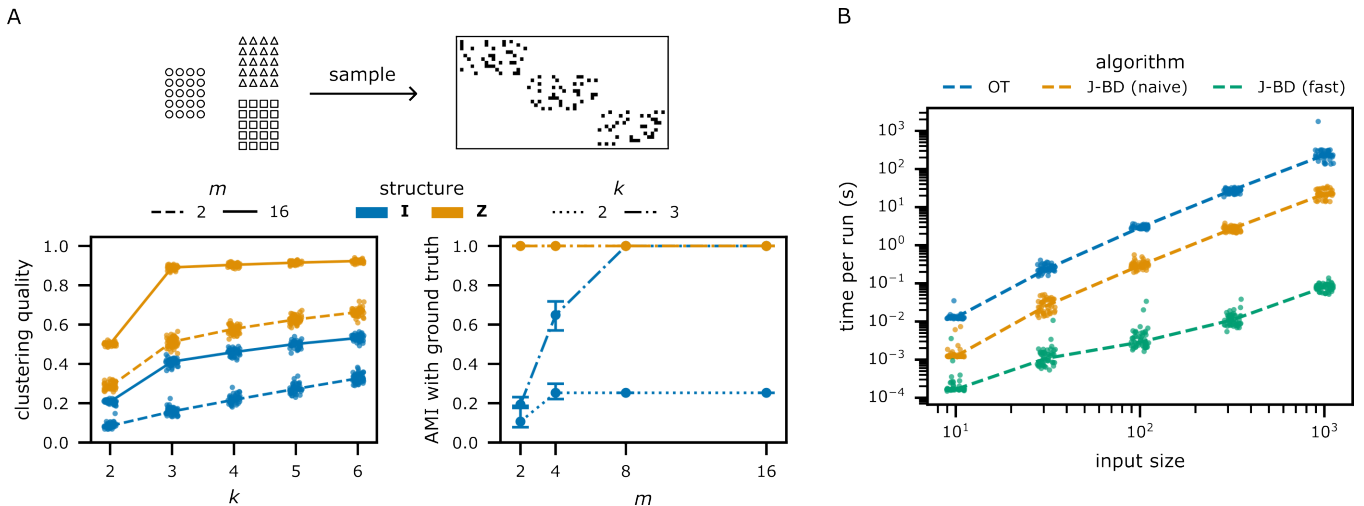


FIG. 2. **Synthetic experiments.** **A. Planted patterns.** (Top) The embedding in \mathbb{R}^2 , with ground truth groups represented as different shapes. We show a typical sample with $m = 4$, with each row corresponding to a distribution. (Bottom left) The clustering quality as a function of k for **I** (blue) and **Z** (orange). The points mark the results from 50 runs and the lines connect the median values for $m = 2$ (dashed) and $m = 16$ (solid). (Bottom right) The alignment with ground truth, measured using Adjusted Mutual Information (AMI), against m . We report the median and 95% confidence intervals for $k = 2$ (dotted) and $k = 3$ (dot-dashed). **B. Runtime.** The runtime in seconds as a function of the number of input distributions for the all-pairs dissimilarity task. The points mark the results from 50 runs each for OT (blue), J-BD (naive) (orange), and J-BD (fast) (green). The lines connect the medians. The J-BD methods use $\alpha = 2$. Note the log scale on both axes.

to similar sectors, but may require very different skills. For instance, the occupations most similar to *Agricultural and Related Trades* by co-location are *Animal Care and Control Services*, *Veterinary nurses*, and *Managers and Proprietors in Agriculture Related Services*. However, the latter is ranked 20th out of 40 by skills similarity. The most skills similar occupation is *Elementary Storage Occupations*, which is ranked 26th by co-location.

How does incorporating relatedness alter the comparison of LAs? The entropy of an LA’s occupational composition measures the diversity of its capability base. Setting $\alpha = 2$ to align with Daniotti et al. [5], Kendall’s τ between diversity rankings is 0.63 (no similarity vs skills), 0.68 (no similarity vs co-location), and 0.54 (skills vs co-location). The divergence of an LA’s occupational composition from the population’s indicates how representative it is: atypical LAs have high values. The corresponding Kendall’s τ values are 0.79, 0.80, and 0.90 respectively (see SI Appendix for other values of α).

1. Regionalisation

Grouping LAs into regions with similar capability bases reveals broad patterns in specialisation. The two-way partitions are similar for all choices of **Z** and explain a large fraction of the Bregman information (Fig. 3). This division captures the concentration of white collar employment in the south east surrounding London and in small pockets around cities such as Manchester, Bristol, and Cardiff (see SI Appendix). For larger k , the optimal partitions can be quite different, as we illustrate for $k = 3$

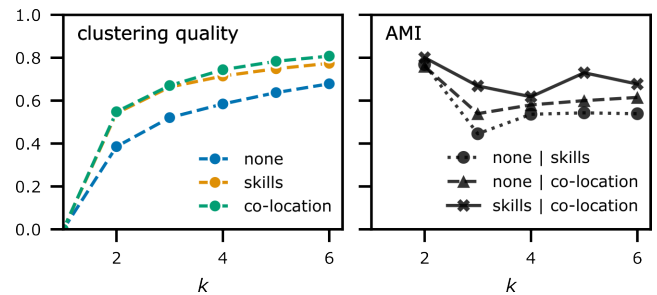


FIG. 3. **Statistics for regionalisation by occupational composition.** (Left) Clustering quality as a function of the number of clusters k for occupation similarity matrices modelling no similarity (blue), skills similarity (orange), and co-location similarity (green). The clustering quality of a partition is the fraction of total Bregman information explained by it. (Right) The AMI between the optimal partitions for each k for each pair of similarity matrices.

in Fig. 4.

All three partitions reveal a services-heavy region primarily in the south east (dark shade, Fig. 4). This region is similar in the structure-aware partitions (orange for skills and green for co-location), and contains around 25% of the population. It is substantially larger in the structure-blind partition (blue), with more than 33% of the population. The remaining regions differ markedly depending on the definition of similarity.

Using co-location similarity reveals sector-specialised regions. The industry-heavy region (medium green) includes population centres such as Birmingham,

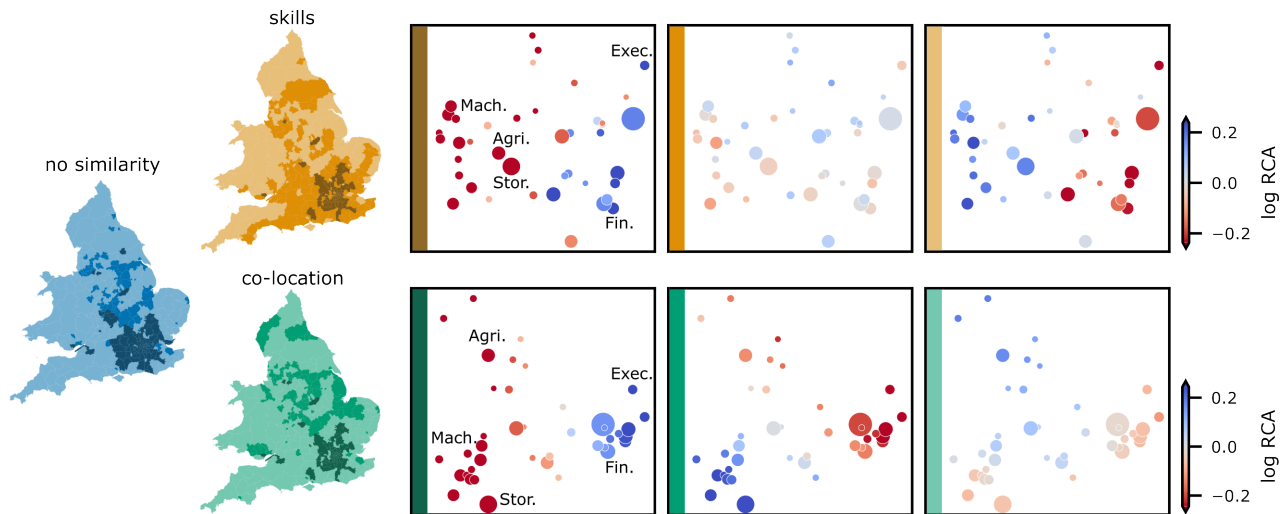


FIG. 4. **Three-way partitions by occupational composition.** (Left) The geography of the optimal partitions into three regions using no occupation similarity (blue), skills similarity (orange), and co-location similarity (green). We distinguish the regions by intensity of colour (light, medium, and dark). (Right) The occupational composition of each cluster for skills (top row) and co-location (bottom row) similarity. Each point is an occupation, with size corresponding to employment share in the total population. We label a few distinctive occupations (see end of caption for abbreviations). Their positions are set by Multi-Dimensional Scaling (MDS) of the similarity structure – similar occupations are closer. Each plot corresponds to the region indicated by the stripe on its left margin. The colour of an occupation represents the Revealed Comparative Advantage (RCA) of the corresponding region in it. Blue and red indicate over and under-representation respectively. Abbreviations: Exec. is *Chief Executives and Senior Officials*, Fin. is *Finance Professionals*, Mach. is *Plant and Machine Operatives*, Stor. is *Elementary Storage Occupations*, and Agri. is *Agricultural and Related Trades*.

Northamptonshire, and Bradford and houses 30% of the population. The vast agricultural region (light green) spans nearly half the LAs and 43% of the population, encompassing nearly all of Yorkshire, Cornwall, and Wales.

Under skill similarity, some industrial and agricultural LAs merge into one region (light orange) with 38% of the population. An interpretation of skills-based regions is that two LAs are in the same region if the workforce of one can perform the occupations of the other. The overlap in the skills of blue collar occupations across sectors means that LAs with large population shares in them are grouped together. The remaining skill-based region has no clear specialisation (medium orange). Despite having 37% of the population, it contributes only 0.8% to the 66% of information explained by the partition, indicating that on average, it is very typical of the overall population.

These differences show that clustering based on structure-aware divergence is sensitive to the similarity structure in intuitive ways. In economic geography, this enables regionalisation under different notions of relatedness. The usefulness of the resulting regions depends on how well the similarity structure aligns with the research question.

G. β -diversity of vegetation in the Rutor glacier

The variability of ecosystem composition across sampling sites, termed β -diversity, is a vital quantity in ecology [40, 41]. A key step in defining β -diversity is deciding how to measure the difference between sites. A growing body of research advocates for incorporating species similarities, defined using traits that proxy their functional role in the ecosystem [12, 13]. Researchers argue that functional β -diversity is a better signal of ecological processes.

Ricotta et al. [42] proposed a functional β -diversity measure built on Gregorius et al.’s OT approach to comparing trait distributions [43]. Broadly, this method matches species between two sites in order to minimise the mean dissimilarity between pairs of matched individuals. This comes at a computational cost, which is remarked upon by Ricotta et al. We show that our framework reproduces the insights of Ricotta et al. [42] and Ricotta and Pavoine [44] on functional β -diversity in the distribution of vegetation in the Rutor glacier.

The data consists of the abundances and functional traits of 45 plant species in 59 plots along the glacier [45]. We use the traits to define a similarity matrix \mathbf{Z} between the species (see Methods). The plots are along a primary succession, where the retreating glacier exposed previously uninhabited soil. They come from three different successional stages defined using the age of the glacial deposits. There are 17 early, 32 mid, and 10

late stage plots. Previous studies [42, 44] found that while species turnover amongst plots is comparable for the three stages, the mid and late stages have much lower functional β -diversity than the early stage. This indicates that while species vary amongst the plots in the mid and late stages, their functional composition remains fairly similar. Plots from the early stage are more functionally different.

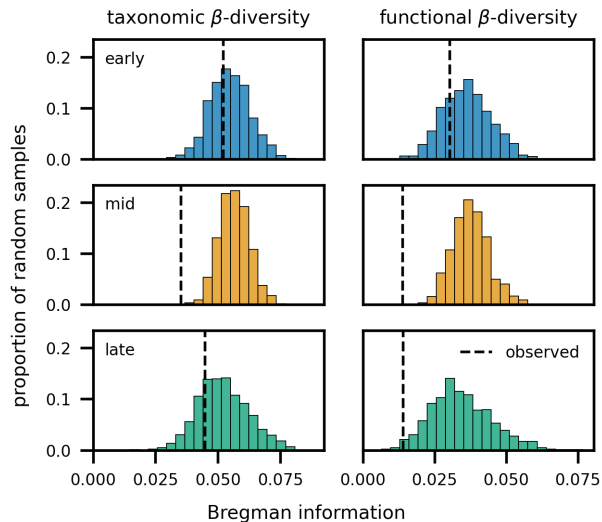


FIG. 5. β -diversity of the successional stages of the Rutor glacier. We plot the taxonomic (left) and functional (right) β -diversity of the three successional stages (rows). We measure the β -diversity of a stage as its Bregman information. The distributions are the β -diversities of 1,000 synthetic stages with randomly sampled plots. The dashed black lines mark the empirical values. These results are for $\alpha = 2$.

We measure the β -diversity of a stage as its Bregman information assuming a uniform distribution over the plots. Using \mathbf{I} captures species turnover or taxonomic β -diversity and using \mathbf{Z} the functional β -diversity. We set $\alpha = 2$ for this analysis. For each stage, we compare the empirical β -diversity to a null model where we generate 1,000 synthetic stages with the same number of plots sampled uniformly at random. If a stage were comprised of similar plots, we would expect its β -diversity to be lower than the null model.

The taxonomic β -diversities of the mid and late stages are 67% and 86% respectively of the early stage's (Fig. 5). Their functional β -diversities are both 46% of the early stage's. This supports the theory that random dispersal mechanisms drove early colonisation while biotic interactions shaped the later stages [42, 44]. The early stage plots are not significantly taxonomically or functionally similar than at random. Of the 1,000 randomly sampled subsets of 17 plots, 39% (taxonomic) and 24% (functional) have a lower β -diversity than the early stage. The mid stage is more cohesive taxonomically and functionally than at random. Interestingly, while 24% of the random subsets have a lower taxonomic β -diversity than the

late stage, only 1% are less functionally diverse. These results are qualitatively identical for $\alpha = 3$ and 4, indicating that they are not driven by the rare species (see SI Appendix).

III. DISCUSSION

Similarity relations within a distribution's support frequently play a central role in modelling and inference. The conventional assumption that outcomes are either the same or wholly distinct, though convenient, eliminates potentially informative structure. Standard information theory measures including Shannon entropy [15] and KL divergence [20] do not account for similarity. While structure-aware entropies have been explored in multiple fields, we advance the literature by introducing a structure-aware divergence for comparing distributions.

Our work builds on the diversity measures defined by Ricotta and Szeidl [26]. We show that they are strictly concave under certain conditions and provide a wide range of useful examples that satisfy them. This allows us to define structure-aware divergences [31] using the geometric machinery of Bregman divergences that connect KL divergence and Shannon entropy. The corresponding Bregman information is the analogue of mutual information [32].

With a synthetic clustering experiment, we show that (i) some patterns are irretrievably lost by discarding structure, and (ii) modelling structural information helps us recover planted patterns with less sampling than structure-blind methods. In a separate experiment, we compare our tools to the OT approach [28] to comparing distributions over structured spaces. Our closed form expression makes computing structure-aware divergence at least an order of magnitude faster, with vectorising yielding more gains.

We demonstrate the applicability of our methods to real systems with examples from economic geography and ecology, where both theory and empirics have established the importance of structure [6, 13]. Motivated by recent research studying occupational composition with structure-aware entropy [5], we study the geography of occupations in England and Wales. We find that structure changes the rankings of locations by occupation diversity and representativeness. Structure-aware regionalisation reveals clusters that depend on the choice of similarity measure in intuitive ways. The importance of relatedness in explaining processes such as diversification and innovation [2, 3, 6] suggests that our methods are broadly applicable.

Data-driven regionalisation also provides insights into segregation [46], allowing researchers to combat the modifiable areal unit problem. In previous work [47], we measured ethnic segregation in England and Wales at different administrative scales. Following information theory-based segregation research [48, 49], we moved between demographic scales by merging ethnic groups. The

methods we propose here allow us to move past this binary choice and are compatible with recent regionalisation methods [50]. Evidence that perceptions of diversity are subjective [51, 52] suggests that this flexibility is needed.

In an ecology case study, we compared Bregman information to an OT formulation of functional β -diversity [42, 43]. Our results are qualitatively identical to previous studies [42, 44] of vegetation in the Rutor glacier. To our knowledge, the numerical value of the OT-based β -diversity is not biologically interpretable: its purpose is to enable comparison. This suggests that our methods reduce computational costs without sacrificing interpretability. Scalability is likely to become increasingly important as large datasets of species abundances and traits become more common [53, 54].

Several avenues for methodological research emerge from our work. On the mathematical side, our conditions for the strict concavity of $\mathcal{H}_\alpha^{\mathbf{Z}}$ are sufficient but not necessary; relaxing them would extend the applicability of our methods. Schoenberg [55] constructed positive semidefinite similarity kernels from metrics with a wider class of ‘completely monotone’ functions, which may be useful for our methods. From a geometric perspective, Bregman divergences admit well-behaved projections onto subsets of the probability simplex [33], opening up applications that we have not yet explored. Computational challenges also arise for large n : storing and manipulating a dense similarity matrix may be infeasible, and developing sparse or approximate representations would improve scalability. Extending our clustering algorithm to allow soft clusters [32] would make it more versatile. In conclusion, our structure-aware divergences provide a broadly applicable framework for analysing distributions, while opening avenues for further methodological development.

IV. METHODS

A. Structure-aware entropy

Our definition of $\mathcal{H}_\alpha^{\mathbf{Z}}$ is due to Leinster and Cobbold [25], who proved that it is equivalent to Ricotta and Szeidl’s [26] original formulation. For $\mathbf{Z} = \mathbf{I}$, we recover a family of entropies parametrised by α , originally proposed by Havrda and Charvát [17], and known in statistical physics after Tsallis [56] and in ecology after Patil and Taillie [19]. How does $\mathcal{H}_\alpha^{\mathbf{Z}}$ depend on its parameters?

Proposition 1. Increasing similarity decreases entropy. $\mathbf{Z}_1 \geq \mathbf{Z}_2 \implies \mathcal{H}_{\alpha_1}^{\mathbf{Z}_1} \leq \mathcal{H}_{\alpha_2}^{\mathbf{Z}_2}$.

Leinster and Cobbold proved this property for structure-aware Hill numbers [25, Appendix Proposition A17]. Our proposition follows since given α , $\mathcal{H}_\alpha^{\mathbf{Z}}$ is an invertible and increasing transformation of the structure-aware Hill numbers. $\mathcal{H}_\alpha^{\mathbf{Z}}$ is highest for $\mathbf{Z} = \mathbf{I}$.

Proposition 2. Increasing α decreases entropy. $\alpha_1 \geq \alpha_2 \implies \mathcal{H}_{\alpha_1}^{\mathbf{Z}} \leq \mathcal{H}_{\alpha_2}^{\mathbf{Z}}$.

In the SI Appendix, we show that increasing α reduces the surprise (Eq. 5) of each element. Rarer elements are affected more. Thus, choosing α can be viewed as picking the sensitivity to rare elements.

B. Strict concavity of $\mathcal{H}_\alpha^{\mathbf{Z}}$

Given $\mathbf{Z} \succ 0$ and $\alpha \geq 2$, we will show that $\mathcal{H}_\alpha^{\mathbf{Z}}$ is strictly concave in Δ_n° (Thm. 1). We use the second derivative test [57, Section 3.1.4].

Lemma 1. Let $\phi : \Omega \rightarrow \mathbb{R}$ be a twice-differentiable function on an open convex domain Ω .

$$\nabla^2 \phi(\omega) \prec 0 \forall \omega \in \Omega \implies \phi \text{ is strictly concave}$$

Let us first establish that $\mathcal{H}_\alpha^{\mathbf{Z}}$ satisfies the conditions of the lemma. Δ_n° is indeed open and convex. For $\alpha \geq 2$, $\mathcal{H}_\alpha^{\mathbf{Z}}$ is a generalised multivariate polynomial in the entries of \mathbf{p} , ensuring that it is twice-differentiable for $\mathbf{p} \in \Delta_n^\circ$.

We define diagonal matrices

$$\begin{aligned} \mathbf{D}_1 &= \text{diag} \left((\mathbf{Z}\mathbf{p})^{\alpha-2} \right) \\ \mathbf{D}_2 &= \text{diag} \left(\mathbf{p} \otimes (\mathbf{Z}\mathbf{p})^{\alpha-3} \right), \end{aligned}$$

where the powers are element-wise, \otimes is element-wise multiplication, and we drop the explicit dependence on \mathbf{p} . The gradient and the Hessian are as follows.

$$\nabla \mathcal{H}_\alpha^{\mathbf{Z}}(\mathbf{p}) = -\frac{1}{\alpha-1} (\mathbf{Z}\mathbf{p})^{\alpha-1} - \mathbf{Z}\mathbf{D}_1\mathbf{p}$$

$$\nabla^2 \mathcal{H}_\alpha^{\mathbf{Z}}(\mathbf{p}) = -(\mathbf{Z}\mathbf{D}_1 + \mathbf{D}_1\mathbf{Z} + (\alpha-2)\mathbf{Z}\mathbf{D}_2\mathbf{Z})$$

From the definition of negative definiteness, $\nabla^2 \mathcal{H}_\alpha^{\mathbf{Z}}(\mathbf{p}) \prec 0$ if $\mathbf{x}^\top \nabla^2 \mathcal{H}_\alpha^{\mathbf{Z}}(\mathbf{p}) \mathbf{x} < 0$ for $\mathbf{x} \in \mathbb{R}^n \setminus \{\mathbf{0}\}$.

$$\begin{aligned} \mathbf{x}^\top \nabla^2 \mathcal{H}_\alpha^{\mathbf{Z}}(\mathbf{p}) \mathbf{x} &= -\mathbf{x}^\top (\mathbf{Z}\mathbf{D}_1 + \mathbf{D}_1\mathbf{Z} + (\alpha-2)\mathbf{Z}\mathbf{D}_2\mathbf{Z}) \mathbf{x} \\ &= -2 \left(\mathbf{D}_1^{1/2} \mathbf{x} \right)^\top \mathbf{Z} \left(\mathbf{D}_1^{1/2} \mathbf{x} \right) \\ &\quad - (\alpha-2) \left(\mathbf{D}_2^{1/2} \mathbf{Z}\mathbf{x} \right)^\top \left(\mathbf{D}_2^{1/2} \mathbf{Z}\mathbf{x} \right) \end{aligned}$$

First term: $(\mathbf{Z}\mathbf{p})_i > 0$ since \mathbf{Z} is a similarity matrix and $\mathbf{p} \in \Delta_n^\circ$. Therefore, $\mathbf{D}_1^{1/2}$ is a diagonal matrix with positive diagonal and is invertible, i.e. $\mathbf{D}_1^{1/2} \mathbf{x} \neq \mathbf{0}$ for $\mathbf{x} \neq \mathbf{0}$. The first term is negative since $\mathbf{Z} \succ 0$.

Second term: The inner product is a Euclidean norm and we have $\alpha \geq 2$. Thus, the second term is non-negative.

Together, this guarantees that the Hessian is negative definite. Thus, by the lemma, $\mathcal{H}_\alpha^{\mathbf{Z}}$ is strictly concave.

More general conditions The theorem is a one-way implication. Potentially useful ways to relax the conditions include the following.

- The Hessian only needs to be negative definite in Δ_n^o . Thus, we only need $\mathbf{x}^\top \nabla^2 \mathcal{H}_\alpha^{\mathbf{Z}}(\mathbf{p}) \mathbf{x} < 0$ for $\mathbf{x} \in \{\mathbf{x} \in \mathbb{R}^n \mid \mathbf{1}^\top \mathbf{x} = 0\} \setminus \{\mathbf{0}\}$.
- Establishing bounds on the two terms of the quadratic form may help to relax the conditions on α (see Posada et al.’s [58] conjecture for $\alpha = 1$).

C. Positive definite similarity matrices

1. From metrics

Let $\mathbf{D} \in \mathbb{R}^{n \times n}$ be the distance matrix of a metric on \mathcal{X} . The transformation $Z_{ij} = \exp(-D_{ij})$ has been long-studied the geometry of embeddings [55] and more recently in the theory of magnitude [36, 59].

Definition 7. A finite metric space with distance matrix \mathbf{D} is **stably positive semidefinite** if the similarity matrix \mathbf{Z} with entries $Z_{ij} = \exp(-\tau D_{ij})$ is positive semidefinite for all $\tau > 0$. It is **stably positive definite** if $\mathbf{Z} \succ 0$ for all $\tau > 0$.

Meckes [36, Theorem 3.3] showed that these two definitions coincide and are equivalent to the metric space being of negative type [55].

Definition 8. A finite metric space with distance matrix \mathbf{D} is of **negative type** if

$$\mathbf{v}^\top \mathbf{D} \mathbf{v} \leq 0 \quad \forall \mathbf{v} \in \{\mathbf{v} \in \mathbb{R}^n \mid \mathbf{1}^\top \mathbf{v} = 0\}. \quad (9)$$

Further, it is of **strictly negative type** if equality is achieved only at $\mathbf{v} = \mathbf{0}$.

An equivalent definition for negative type is $\mathbf{D}^{1/2}$ being isometric to a subset of a Hilbert space. Many useful metric spaces are of the negative type. For more examples beyond those in our Results section, we refer to Meckes [36, Theorem 3.6]. In the SI Appendix, we show that a broad class of similarity matrices defined using hierarchies are guaranteed to be positive definite. We also find that for a metric where each element has the same mean distance from the others, distances can be converted to similarities linearly. While this is unlikely in real systems, our proof might inspire a way to relax the condition.

2. From other similarity matrices

Suppose we have a similarity matrix $\mathbf{M} \neq \mathbf{0}$. If $\mathbf{M} \succeq 0$, we can use the simple transformation $\mathbf{M} \mapsto \delta \mathbf{I} + (1 - \delta) \mathbf{M}$ for $\delta \in (0, 1]$. This raises the minimum eigenvalue to δ while preserving the range and symmetry conditions.

For a more principled approach that works for general \mathbf{M} , we can frame finding the nearest positive definite similarity matrix as a convex optimisation problem [57]. The goal is to minimise the squared Frobenius norm $\|\mathbf{Z} - \mathbf{M}\|_F^2$, such that \mathbf{Z} is a similarity matrix and $\mathbf{Z} \succ 0$. The constraints $Z_{ij} \in [0, 1]$ are so-called ‘box’ constraints and are convex, as is $Z_{ii} = 1$. If we want to ensure that the off-diagonals are strictly less than 1, we can restrict them to $[0, 1 - \epsilon]$ for some $\epsilon > 0$. Since the set of positive definite matrices is open, $\mathbf{Z} \succ 0$ is not a convex constraint. In practice, we can require $\mathbf{Z} - \delta \mathbf{I} \succeq 0$ for some $\delta > 0$, thereby ensuring that the smallest eigenvalue of \mathbf{Z} is at least δ . This restricts \mathbf{Z} to be in a translation of the positive semidefinite cone, which is convex. The convex optimisation problem can be solved with semidefinite programming [60] or projection methods [61].

D. Bregman information

For a weighted set of distributions, a best representative is the distribution from which the mean divergence of the set is minimised. For Bregman divergences, the mean is the unique best representative [32]. The corresponding minimum expected divergence is Bregman information. Banerjee, Guo, and Wang proved that along with some mild regularity conditions, the mean-minimiser property characterises Bregman divergences [62, Theorem 4]. Bregman information is also the Jensen gap of negative entropy. Chodrow showed that this equivalence characterises Bregman divergences [63, Theorem 1].

E. Clustering

For a partition of a set of distributions, we can write the total Bregman information as a sum of between and within-cluster components [32]. This is exactly the decomposition of variance used by k-means clustering and allows us to identify the contribution of each cluster. Good partitions maximise between-cluster information and the k-means-style algorithm of alternately updating centroids and cluster assignments finds locally optimal partitions. We provide code to perform clustering in our software release.

F. Synthetic experiments

1. Recovering planted partitions

The elements are embedded in the integer lattice in groups as shown in Fig. 2. We construct \mathbf{Z} by computing the Manhattan distance d and mapping $d \mapsto \exp(-d)$. Manhattan distance is of negative type [36]. To generate a distribution from a group, we sample m elements from it with replacement. Since we need non-zero probabilities, we smooth the sampled distribution

as $\mathbf{p} \mapsto 0.95\mathbf{p} + 0.05\mathbf{u}$, where \mathbf{u} is the uniform distribution over all 60 elements.

A single run of the experiment involves clustering 30 distributions: ten each from the three groups. We perform 50 runs each for $m \in \{2, 4, 8, 16\}$. We use a k-means style algorithm to cluster the distributions for $k \in [2, 6]$. In Fig. 2A, we report the fraction of Bregman information explained by the clustering and the Adjusted Mutual Information (AMI) with the ground truth at $k = 2$ and 3. Our software release contains the code for these experiments.

2. Runtime compared to Optimal Transport

For the OT solution to the all-pairs dissimilarity task, we compute the Wasserstein-1 distance as implemented by the `emd2` function [64] of the state-of-the-art Python library POT [65]. For our J-BD approaches, we define dissimilarity as Jensen-Bregman divergence. In OT and J-BD (naive), we iterate over each pair. In J-BD (fast), we use a vectorised algorithm optimised for the task. We do not benchmark against OT algorithms that compute approximate solutions since their speed and quality are sensitive to parameters that we have no clear way of choosing.

In a run of input size n , we sample n distributions over 50 elements uniformly at random from Δ_{50}° . We generate structure by sampling an embedding for each element uniformly at random from the 10-cube $[0, 1]^{10}$ with the Euclidean metric. OT works directly with distances. For J-BD, we construct \mathbf{Z} by mapping distances as $d \mapsto \exp(-d)$ and set $\alpha = 2$ (see SI Appendix for $\alpha = 3$). For each run, we track the time taken and the Pearson’s r and Kendall’s τ between the OT and J-BD dissimilarities. We conduct 50 runs each for five values of $n \in [10, 10^3]$. Note that the output size scales as the square of the input size.

We run all the algorithms on a standard laptop in the same Python environment with standard libraries. Our software release contains the code to run these experiments.

G. The geography of occupations in England and Wales

1. Data

Census 2021 data for England and Wales was collected and is maintained by the Office for National Statistics (ONS) and provided through Nomis. We obtain occupation data from Table TS064, which records the occupation of residents aged 16 years and over [66]. We pick the Local Authority (LA) level for geography (*local authorities: district / unitary (as of April 2023)* on Nomis). We obtain the geography shapefile from the ONS [67].

2. Tradable occupations

Some occupations such as teachers, retail workers, and health service staff cater primarily to local population. The employment in these ‘non-tradable’ occupations scales roughly with population. To characterise regions, we focus on tradable occupations, whose share of the labour force reveals what the region specialises in. Examples include manufacturing and agriculture, as well as services such as legal and finance professions. We follow the methodology of Daniotti et al. [5] to identify the tradable occupations in England and Wales.

We start with 104 occupations encoded at the 3 digit level of the Standard Occupational Classification (SOC) 2020. To quantify the tradability of occupation i , we measure correlation between the distributions of i ’s workers and all workers over LAs. A high Pearson’s r indicates that i employs similar shares of the labour force in each LA. We define tradability as $1 - r$ [5]. The Spearman’s rank correlation between tradability and Krugman’s locational Gini coefficient is 0.97, indicating that the latter would rank occupations almost identically (see SI Appendix).

Picking a threshold of 0.2, we retain 42 occupations that employ 24.2% of the workforce (see SI Appendix Fig. S2). Additionally, we drop *Bed and Breakfast and Guest House Owners and Proprietors* since it has no employment in several LAs. It is the smallest of the tradable occupations and only employs 7,354 people (0.026% of the workforce). This leaves us with 41 occupations (SI Appendix Table S1).

3. Similarity matrices

We define skills similarity with the ONET mapping of occupations to importance ratings between 1 and 5 for each of 35 skills [68]. We use the National Foundation for Educational Research (NFER) mapping to connect SOC2020 to ONET occupation codes [69] and aggregate up to 3 digit level. Each of our occupations is linked to multiple ONET occupations and we embed them in \mathbb{R}^{35} by computing their mean skill vector. We transform Euclidean distance d into similarities using $d \mapsto \exp(-\tau d)$ and pick τ such that the median similarity between occupations is 0.1. For more details, see the SI Appendix and our software release.

To define co-location similarity, we compute the Revealed Comparative Advantage (RCA) [70] of LA l in occupation i as

$$\text{RCA}(i, l) = \frac{n_{il}/n_{\cdot l}}{n_{i\cdot}/n_{\cdot\cdot}}, \quad (10)$$

where n_{il} is the number of people in l that work in i and \cdot indicates a sum over the index. $\text{RCA}(i, l)$ is the ratio of i ’s share in the workforce of l to i ’s share of the overall workforce. We consider occupations as similar if LAs have similar RCA in them. To avoid noise

from small population sizes, we restrict the comparison to the 100 most populous LAs. We embed each occupation in \mathbb{R}^{100} as the vector of the log RCA of the LAs in it. We transform Euclidean distance d into similarities using $d \mapsto \exp(-\tau d)$ with median similarity 0.1.

4. Clustering

We employ a k-means-style algorithm for clustering. Each LA is modelled as its distribution over the 41 tradable occupations and weighed by its share of the population. Starting from k initial cluster centres, we alternatively update cluster assignments and centres until convergence. We report the best partition out of 100 trials with random initialisations. Our clustering is not explicitly geographical: we do not require clusters to be contiguous. See Chodrow [50] for Bregman information-based regionalisation with spatial constraints.

H. β -diversity of vegetation in the Rutor Glacier

1. Data

We use data on the abundance and traits of vegetation in the Rutor glacier in Italy. The data was originally collected by Caccianiga et al. [45] and we accessed it using the R package `adiv` [71]. The data consists of the relative abundances of 45 species of plants in 59 plots along a primary succession. Based on the age of the glacial deposits, Caccianiga et al. grouped the plots into three successional stages: early (17), mid (32), and late (10). The species traits we use are canopy height, leaf dry mass content, leaf dry weight, specific leaf area, leaf nitrogen content, and leaf carbon content. For more details, see

Caccianiga et al. [45].

2. Similarity matrix

We follow Ricotta et al. [42] exactly to define species similarity. We standardise the six traits listed above to zero mean and unit standard deviation. We compute the Euclidean distance matrix between the species and linearly re-scale it such that the maximum distance is 1. We map these distances into similarities using $d \mapsto 1 - d$. In this case, the mapping produces a positive definite \mathbf{Z} .

DATA AND SOFTWARE AVAILABILITY

We provide code to implement our methods and reproduce our experiments at <https://github.com/rohit-sahasrabudde/structure-aware-divergence>. All the data we use is public and included in the repository.

ACKNOWLEDGEMENTS

We thank Karel Devriendt for many useful discussions. We are grateful to the teams maintaining the open source data and software that we use. R.S. is funded by the Mathematical Institute at the University of Oxford. R.L. acknowledges support from the EPSRC grants EP/V013068/1, EP/V03474X/1, and EP/Y028872/1.

AUTHOR CONTRIBUTIONS.

R.S.: Conceptualisation, Methodology, Software, Investigation, Writing - Original Draft, Writing - Review and Editing.

R.L.: Conceptualisation, Investigation, Writing - Review and Editing.

-
- [1] C. A. Hidalgo, B. Klinger, A.-L. Barabaási, and R. Hausmann. The product space conditions the development of nations. *Science*, 317:482–487, 7 2007.
 - [2] Koen Frenken, Frank Van Oort, and Thijs Verburg. Related variety, unrelated variety and regional economic growth. *Regional Studies*, 41:685–697, 7 2007.
 - [3] Frank Neffke, Martin Henning, and Ron Boschma. How do regions diversify over time? industry relatedness and the development of new growth paths in regions. *Economic Geography*, 87:237–265, 7 2011.
 - [4] Luís M. A. Bettencourt, Horacio Samaniego, and Hyejin Youn. Professional diversity and the productivity of cities. *Scientific Reports*, 4:5393, 6 2014.
 - [5] Simone Daniotti, Matté Hartog, and Frank Neffke. The coherence of US cities. *Proceedings of the National Academy of Sciences of the United States of America*, 122:2501504122, 9 2025.
 - [6] César A. Hidalgo, Pierre-Alexandre Balland, Ron Boschma, Mercedes Delgado, Maryann Feldman, Koen Frenken, Edward Glaeser, Canfei He, Dieter F. Kogler, Andrea Morrison, Frank Neffke, David Rigby, Scott Stern, Siqi Zheng, and Shengjun Zhu. *The Principle of Relatedness*, volume 0, pages 451–457. Springer Science and Business Media B.V., 2018.
 - [7] Lou Jost. Entropy and diversity. *Oikos*, 113:363–375, 5 2006.
 - [8] Aisling J. Daly, Jan M. Baetens, and Bernard De Baets. Ecological diversity: Measuring the unmeasurable. *Mathematics*, 6:119, 7 2018.
 - [9] Tom Leinster. *Entropy and Diversity*. Cambridge University Press, 4 2021.
 - [10] Sandra Díaz and Marcelo Cabido. Vive la différence: plant functional diversity matters to ecosystem processes. *Trends in Ecology & Evolution*, 16:646–655, 11 2001.

- [11] David Tilman. *Functional Diversity*, pages 587–596. Elsevier, 2001.
- [12] Cyrille Violle, Marie Laure Navas, Denis Vile, Elena Kazakou, Claire Fortunel, Irène Hummel, and Eric Garnier. Let the concept of trait be functional! *Oikos*, 116:882–892, 5 2007.
- [13] Brian J. McGill, Brian J. Enquist, Evan Weiher, and Mark Westoby. Rebuilding community ecology from functional traits. *Trends in Ecology and Evolution*, 21:178–185, 4 2006.
- [14] Thomas M. Cover and Joy A. Thomas. *Elements of Information Theory*. Wiley, 9 2005.
- [15] C. E. Shannon. A mathematical theory of communication. *Bell System Technical Journal*, 27:379–423, 7 1948.
- [16] Alfréd Rényi. On measures of entropy and information. In *Proceedings of the fourth Berkeley symposium on mathematical statistics and probability, volume 1: contributions to the theory of statistics*, volume 4, pages 547–562. University of California Press, 1961.
- [17] Jan Havrda and František Charvát. Quantification method of classification processes. concept of structural α -entropy. *Kybernetika*, 03:(30)–35, 1967.
- [18] M. O. Hill. Diversity and evenness: A unifying notation and its consequences. *Ecology*, 54:427–432, 3 1973.
- [19] G. P. Patil and C. Taillie. Diversity as a concept and its measurement. *Journal of the American Statistical Association*, 77:548, 9 1982.
- [20] S. Kullback and R. A. Leibler. On information and sufficiency. *The Annals of Mathematical Statistics*, 22:79–86, 3 1951.
- [21] Imre Csiszár. Information-type measures of difference of probability distributions and indirect observation. *Studia Scientiarum Mathematicarum Hungarica*, 2:299–318, 1967.
- [22] Shun’ichi Amari. *Information geometry and its applications*. Applied mathematical sciences, volume 194. Springer, Japan, 2016.
- [23] C. Radhakrishna Rao. Diversity and dissimilarity coefficients: A unified approach. *Theoretical Population Biology*, 21:24–43, 2 1982.
- [24] Karel Devriendt, Samuel Martin-Gutierrez, and Renaud Lambiotte. Variance and covariance of distributions on graphs. *SIAM Review*, 64:343–359, 5 2022.
- [25] Tom Leinster and Christina A. Cobbold. Measuring diversity: the importance of species similarity. *Ecology*, 93:477–489, 3 2012.
- [26] Carlo Ricotta and Laszlo Szeidl. Towards a unifying approach to diversity measures: Bridging the gap between the Shannon entropy and Rao’s quadratic index. *Theoretical Population Biology*, 70:237–243, 11 2006.
- [27] Gaspard Monge. Mémoire sur la théorie des déblais et des remblais. *Histoire de l’Académie Royale des Sciences de Paris, avec les Mémoires de Mathématique et de Physique pour la même année*, pages 666–704, 1781.
- [28] Cédric Villani. *Optimal Transport*, volume 338. Springer Berlin Heidelberg, 2009.
- [29] L. V. Kantorovich. Mathematical methods of organizing and planning production. *Management Science*, 6:366–422, 7 1939.
- [30] Leonid Vaseršteĭn. Markov processes over denumerable products of spaces, describing large systems of automata. *Problemy Peredachi Informatsii*, 5:64–72, 1969.
- [31] L.M. Bregman. The relaxation method of finding the common point of convex sets and its application to the solution of problems in convex programming. *USSR Computational Mathematics and Mathematical Physics*, 7:200–217, 1 1967.
- [32] Arindam Banerjee, Srujana Merugu, Inderjit Dhillon, and Joydeep Ghosh. Clustering with Bregman divergences. In *Proceedings of the 2004 SIAM International Conference on Data Mining*, volume 6, pages 234–245. Society for Industrial and Applied Mathematics, 4 2004.
- [33] Inderjit S. Dhillon and Joel A. Tropp. Matrix nearness problems with Bregman divergences. *SIAM Journal on Matrix Analysis and Applications*, 29:1120–1146, 1 2008.
- [34] Edward Simpson. Measurement of diversity. *Nature*, 163:688–688, 4 1949.
- [35] Prasanta Chandra Mahalanobis. On the generalised distance in statistics. *Proceedings of the National Institute of Sciences of India*, 2:49–55, 1 1936. Reprint online at <https://link.springer.com/article/10.1007/s13171-019-00164-5>.
- [36] Mark W. Meckes. Positive definite metric spaces. *Positivity*, 17:733–757, 9 2013.
- [37] Poul Hjorth, Petr Lisoněk, Steen Markvorsen, and Carsten Thomassen. Finite metric spaces of strictly negative type. *Linear Algebra and its Applications*, 270:255–273, 2 1998.
- [38] Miroslav Fiedler. *Matrices and Graphs in Geometry*. Cambridge University Press, 2 2011.
- [39] K Devriendt. *Graph geometry from effective resistances*. PhD thesis, University of Oxford, 2022.
- [40] R. H. Whittaker. Vegetation of the siskiyou mountains, oregon and california. *Ecological Monographs*, 30:279–338, 7 1960.
- [41] Marti J. Anderson, Thomas O. Crist, Jonathan M. Chase, Mark Vellend, Brian D. Inouye, Amy L. Freestone, Nathan J. Sanders, Howard V. Cornell, Liza S. Comita, Kendi F. Davies, Susan P. Harrison, Nathan J. B. Kraft, James C. Stegen, and Nathan G. Swenson. Navigating the multiple meanings of β diversity: a roadmap for the practicing ecologist. *Ecology Letters*, 14:19–28, 1 2011.
- [42] Carlo Ricotta, Evsey Kosman, Fabien Laroche, and Sandrine Pavoine. Beta redundancy for functional ecology. *Methods in Ecology and Evolution*, 12:1062–1069, 6 2021.
- [43] Hans Rolf Gregorius, Elizabeth M. Gillet, and Martin Ziehe. Measuring differences of trait distributions between populations. *Biometrical Journal*, 45:959–973, 12 2003.
- [44] Carlo Ricotta and Sandrine Pavoine. A new look at functional beta diversity. *Ecological Indicators*, 163:112136, 6 2024.
- [45] Marco Caccianiga, Alessandra Luzzaro, Simon Pierce, Roberta M. Ceriani, and Bruno Cerabolini. The functional basis of a primary succession resolved by csr classification. *Oikos*, 112:10–20, 1 2006.
- [46] Barrett A. Lee, Sean F. Reardon, Glenn Firebaugh, Chad R. Farrell, Stephen A. Matthews, and David O’Sullivan. Beyond the census tract: Patterns and determinants of racial segregation at multiple geographic scales. *American Sociological Review*, 73:766–791, 10 2008.
- [47] Rohit Sahasrabudde and Renaud Lambiotte. Quantifying the spatial and demographic scales of segregation. *arXiv preprint*, 11 2025. <https://arxiv.org/pdf/2511.23069>.
- [48] Sean F. Reardon and Glenn Firebaugh. Measures of

- multigroup segregation. *Sociological Methodology*, 32:33–67, 8 2002.
- [49] Ricardo Mora and Javier Ruiz-Castillo. Entropy-based segregation indices. *Sociological Methodology*, 41:159–194, 8 2011.
- [50] Philip S. Chodrow. Structure and information in spatial segregation. *Proceedings of the National Academy of Sciences of the United States of America*, 114:11591–11596, 10 2017.
- [51] Miguel M. Unzueta and Kevin R. Binning. Which racial groups are associated with diversity? *Cultural Diversity & Ethnic Minority Psychology*, 16:443–446, 7 2010.
- [52] Christopher W. Bauman, Sophie Trawalter, and Miguel M. Unzueta. Diverse according to whom? racial group membership and concerns about discrimination shape diversity judgments. *Personality and Social Psychology Bulletin*, 40:1354–1372, 10 2014.
- [53] Kate E. Jones, Jon Bielby, Marcel Cardillo, Susanne A. Fritz, Justin O’Dell, C. David L. Orme, Kamran Safi, Wes Sechrest, Elizabeth H. Boakes, Chris Carbone, Christina Connolly, Michael J. Cutts, Janine K. Foster, Richard Grenyer, Michael Habib, Christopher A. Plaster, Samantha A. Price, Elizabeth A. Rigby, Janna Rist, Amber Teacher, Olaf R. P. Bininda-Emonds, John L. Gittleman, Georgina M. Mace, and Andy Purvis. PanTHERIA: a species-level database of life history, ecology, and geography of extant and recently extinct mammals. *Ecology*, 90:2648–2648, 9 2009.
- [54] Joseph A. Tobias, Catherine Sheard, Alex L. Pigot, Adam J. M. Devenish, Jingyi Yang, Ferran Sayol, Montague H. C. Neate-Clegg, Nico Alioravainen, Thomas L. Weeks, Robert A. Barber, Patrick A. Walkden, Hannah E. A. MacGregor, Samuel E. I. Jones, Claire Vincent, Anna G. Phillips, Nicola M. Marples, Flavia A. Montañó-Centellas, Victor Leandro-Silva, Santiago Claramunt, Bianca Darski, Benjamin G. Freeman, Tom P. Bregman, Christopher R. Cooney, Emma C. Hughes, Elliot J. R. Capp, Zoë K. Varley, Nicholas R. Friedman, Heiko Korntheuer, Andrea Corrales-Vargas, Christopher H. Trisos, Brian C. Weeks, Dagmar M. Hanz, Till Töpfer, Gustavo A. Bravo, Vladimír Remeš, Larissa Nowak, Lincoln S. Carneiro, Amilkar J. Moncada R., Beata Matysiuková, Daniel T. Baldassarre, Alejandra Martínez-Salinas, Jared D. Wolfe, Philip M. Chapman, Benjamin G. Daly, Marjorie C. Sorensen, Alexander Neu, Michael A. Ford, Rebekah J. Mayhew, Luis Fabio Silveira, David J. Kelly, Nathaniel N. D. Annorbah, Henry S. Pollock, Ada M. Grabowska-Zhang, Jay P. McEntee, Juan Carlos T. Gonzalez, Camila G. Meneeses, Marcia C. Muñoz, Luke L. Powell, Gabriel A. Jamie, Thomas J. Matthews, Oscar Johnson, Guilherme R. R. Brito, Kristof Zyskowski, Ross Crates, Michael G. Harvey, Maura Jurado Zevallos, Peter A. Hosner, Tom Bradfer-Lawrence, James M. Maley, F. Gary Stiles, Hevana S. Lima, Kaiya L. Provost, Moses Chibesa, Mmatjie Mashao, Jeffrey T. Howard, Edson Mlamba, Marcus A. H. Chua, Bicheng Li, M. Isabel Gómez, Natalia C. García, Martin Päckert, Jérôme Fuchs, Jarome R. Ali, Elizabeth P. Derryberry, Monica L. Carlson, Rolly C. Urriza, Kristin E. Brzeski, Dewi M. Prawiradilaga, Matt J. Rayner, Eliot T. Miller, Rauri C. K. Bowie, René-Marie Lafontaine, R. Paul Scofield, Yingqiang Lou, Lankani Somarathna, Denis Lepage, Marshall Illif, Eike Lena Neuschulz, Mathias Templin, D. Matthias Dehling, Jacob C. Cooper, Olivier S. G. Pauwels, Kangkuso Analuddin, Jon Fjeldså, Nathalie Seddon, Paul R. Sweet, Fabrice A. J. DeClerck, Luciano N. Naka, Jeffrey D. Brawn, Alexandre Aleixo, Katrin Böhning-Gaese, Carsten Rahbek, Susanne A. Fritz, Gavin H. Thomas, and Matthias Schleuning. AVONET: morphological, ecological and geographical data for all birds. *Ecology Letters*, 25:581–597, 3 2022.
- [55] I. J. Schoenberg. Metric spaces and positive definite functions. *Transactions of the American Mathematical Society*, 44:522–536, 1938.
- [56] Constantino Tsallis. Possible generalization of boltzmann-gibbs statistics. *Journal of Statistical Physics*, 52:479–487, 7 1988.
- [57] Stephen Boyd and Lieven Vandenberghe. *Convex Optimization*. Cambridge University Press, 3 2004.
- [58] Jose Gallego Posada, Ankit Vani, Max Schwarzer, and Simon Lacoste-Julien. Gait: A geometric approach to information theory. In Silvia Chiappa and Roberto Calandra, editors, *Proceedings of the Twenty Third International Conference on Artificial Intelligence and Statistics*, volume 108 of *Proceedings of Machine Learning Research*, pages 2601–2611. PMLR, 26–28 Aug 2020.
- [59] Tom Leinster. The magnitude of metric spaces. *Documenta Mathematica*, 18:857–905, 1 2013.
- [60] Lieven Vandenberghe and Stephen Boyd. Semidefinite programming. *SIAM Review*, 38:49–95, 3 1996.
- [61] James P. Boyle and Richard L. Dykstra. *A Method for Finding Projections onto the Intersection of Convex Sets in Hilbert Spaces*, pages 28–47. Springer, New York, NY, 1986.
- [62] Arindam Banerjee, Xin Guo, and Hui Wang. On the optimality of conditional expectation as a Bregman predictor. *IEEE Transactions on Information Theory*, 51:2664–2669, 7 2005.
- [63] Philip S. Chodrow. Equivalence of informations characterizes Bregman divergences. *Entropy*, 27:766, 7 2025.
- [64] Nicolas Bonneel, Michiel van de Panne, Sylvain Paris, and Wolfgang Heidrich. Displacement interpolation using lagrangian mass transport. *ACM Transactions on Graphics*, 30:1–12, 12 2011.
- [65] Rémi Flamary, Nicolas Courty, Alexandre Gramfort, Mokhtar Z. Alaya, Aurélie Boisbunon, Stanislas Chambon, Laetitia Chapel, Adrien Corenflos, Kilian Fatras, Nemo Fournier, Léo Gautheron, Nathalie T.H. Gayraud, Hicham Janati, Alain Rakotomamonjy, Ievgen Redko, Antoine Rolet, Antony Schutz, Vivien Seguy, Danica J. Sutherland, Romain Tavenard, Alexander Tong, and Titouan Vayer. Pot: Python optimal transport. *Journal of Machine Learning Research*, 22(78):1–8, 2021.
- [66] Office for National Statistics (ONS). Census 2021 - TS064 - Nomis., 2021. <https://www.nomisweb.co.uk/datasets/c2021ts064>; accessed 05 January, 2026.
- [67] Office for National Statistics (ONS). Local Authority Districts boundaries., 2021. <https://geoportal.statistics.gov.uk/datasets/ons::local-authority-districts-may-2024-boundaries-uk-bfe-2/about>; accessed 05 January, 2026.
- [68] United States Department of Labor. ONET skills mapping, 2026. <https://www.onetcenter.org/dictionary/30.2/excel/skills.html>; accessed 16 March, 2026.
- [69] National Foundation for Educational Research. UK SOC2020 to O*NET2019 systematic mapping, 2026. <https://www.nfer.ac.uk/>

- key-topics-expertise/education-to-employment/
the-skills-imperative-2035/resources/
systematic-mapping-of-soc-2020; accessed 16 March,
2026.
- [70] Bela Balassa. Trade liberalisation and “revealed” com-
parative advantage. *The Manchester School*, 33:99–123,
5 1965.
- [71] Sandrine Pavoine. adiv: An R package to analyse bio-
diversity in ecology. *Methods in Ecology and Evolution*,
11:1106–1112, 9 2020.

Appendix A: Entropy

In the main text, we claimed that picking α can be viewed as choosing the sensitivity to rare elements. First, we will show that increasing α decreases the surprise of every element and therefore the entropy. Let $\sigma : (0, 1) \rightarrow \mathbb{R}$ be the surprise function.

$$\sigma_\alpha(x) = \begin{cases} \frac{1}{\alpha-1} (1 - x^{\alpha-1}) & \text{for } \alpha \neq 1, \\ -\ln x & \text{for } \alpha = 1 \end{cases} \quad (\text{A1})$$

Proposition S1. $\alpha_1 \geq \alpha_2 \implies \sigma_{\alpha_1} \leq \sigma_{\alpha_2}$

Proof. For simplicity, we will only consider the $\alpha \neq 1$ case. The results can be generalised by continuity.

$$\begin{aligned} \frac{d}{d\alpha} \sigma_\alpha(x) &= -\frac{1}{\alpha-1} x^{\alpha-1} \ln x - \frac{1}{(\alpha-1)^2} (1 - x^{\alpha-1}) \\ &= \frac{1}{(\alpha-1)^2} (x^{\alpha-1} (1 - \ln x^{\alpha-1}) - 1), \end{aligned}$$

where we substituted $\ln x = \frac{1}{\alpha-1} \ln x^{\alpha-1}$. Now, since $x \in (0, 1)$, $x^{\alpha-1} (1 - \ln x^{\alpha-1}) < 1$, and therefore, $\frac{d}{d\alpha} \sigma_\alpha < 0$. \square

The surprise of every element decreases when α increases, which proves the Proposition in the main text. Next, we will show that the rarer elements are more affected.

Proposition S2. $x_1 < x_2 \implies \frac{d}{d\alpha} \sigma_\alpha(x_1) < \frac{d}{d\alpha} \sigma_\alpha(x_2)$

Proof.

$$\frac{d}{dx} \left(\frac{d}{d\alpha} \sigma_\alpha(x) \right) = -x^{\alpha-2} \ln x$$

Since $0 < x < 1$, we have $x^{\alpha-2} > 0$ and $\ln x < 0$. Therefore, $\frac{d}{dx} \left(\frac{d}{d\alpha} \sigma_\alpha(x) \right) < 0$. \square

Appendix B: Positive Definite Similarity Matrices

1. Special case: Hierarchies

Suppose we want to define the similarities from a hierarchy. Let us represent the levels of the hierarchy as integers $L = \{0, 1, \dots, l\}$, where 0 is the highest level with a single group and l is the level that the elements of \mathcal{X} belong to.

An intuitive way to construct similarities is from the level at which elements become identical. Let $h(i, j) \in L$ be the level of the lowest common ancestor of the i^{th} and j^{th} elements. Now consider $f : L \rightarrow [0, 1]$ that maps levels to a similarity value. Since $h(i, j) = l$ if and only if $i = j$, we require $f(l) = 1$. Intuitively, elements closer in the hierarchy are more similar, which corresponds to $l_1 \geq l_2 \implies f(l_1) \geq f(l_2)$. A matrix \mathbf{Z} with elements $Z_{ij} = f(h(i, j))$ is guaranteed to be a positive definite similarity matrix.

To prove this, we can represent the hierarchy as a rooted tree and show that each choice of f corresponds to a distribution of edge weights such that the $d \mapsto \exp(-d)$ transformation of the shortest path distance yields the same \mathbf{Z} . In this construction, the weight of all the edges between levels $l - k$ and $l - k + 1$ are identical, and we denote it as $d_{l-k, l-k+1}$. Setting

$$d_{l-k, l-k+1} = \frac{1}{2} \left(\ln \frac{f(l-k+1)}{f(l-k)} \right) \quad (\text{B1})$$

provides the desired \mathbf{Z} . Thus, any reasonable measure of similarity that is constructed from a hierarchy is compatible with our methods. Hierarchical definitions of similarity are convenient in many real systems. For instance, occupation is usually reported using hierarchical classification schemes such as the International Standard Classification of Occupations (ISCO) and the Standard Occupation Classification (SOC), as are industries in the North American Industry Classification System (NAICS) or International Standard Industrial Classification of All Economic Activities (ISIC).

2. Special case: Linear transformation from distance to similarity

Proposition S3. Consider a finite metric space of strictly negative type with distance matrix \mathbf{D} and the similarity matrix \mathbf{Z} with entries

$$Z_{ij} = 1 - \frac{D_{ij}}{\max_{i,j} D_{ij}}.$$

$\mathbf{Z} \succ 0$ if $\mathbf{1}$ is an eigenvector of \mathbf{D} .

Proof. In the following, we will use \mathbf{D} to refer to the rescaled distance matrix. Rescaling does not change the sign of eigenvalues, so \mathbf{D} remains of negative type. Since \mathbf{D} is of strictly negative type,

$$\mathbf{v}^\top \mathbf{D} \mathbf{v} < 0 \quad \forall \mathbf{v} \in \{\mathbf{v} \in \mathbb{R}^n \mid \mathbf{1}^\top \mathbf{v} = 0\} \setminus \{\mathbf{0}\}. \quad (\text{B2})$$

For $\mathbf{Z} = \mathbf{1}\mathbf{1}^\top - \mathbf{D}$, we aim to show that

$$\mathbf{x}^\top \mathbf{Z} \mathbf{x} > 0 \quad \forall \mathbf{x} \in \mathbb{R}^n \setminus \{\mathbf{0}\}. \quad (\text{B3})$$

We begin by noting that $\{\mathbf{v} \in \mathbb{R}^n \mid \mathbf{1}^\top \mathbf{v} = 0\} = \text{span}(\mathbf{1})^\perp$. Thus, we can write any $\mathbf{x} \in \mathbb{R}^n$ as $\mathbf{x} = \mathbf{v} + a\mathbf{1}$ for $\mathbf{v} \in \text{span}(\mathbf{1})^\perp$ and $a \in \mathbb{R}$. Substituting this in the quadratic form above, we get the following.

$$\begin{aligned} \mathbf{x}^\top \mathbf{Z} \mathbf{x} &= (\mathbf{v} + a\mathbf{1})^\top (\mathbf{1}\mathbf{1}^\top - \mathbf{D}) (\mathbf{v} + a\mathbf{1}) \\ &= \mathbf{v}^\top \mathbf{Z} \mathbf{v} + 2a\mathbf{v}^\top \mathbf{Z} \mathbf{1} + a^2 \mathbf{1}^\top \mathbf{Z} \mathbf{1} \end{aligned}$$

Since $\mathbf{v}^\top \mathbf{1}\mathbf{1}^\top \mathbf{v} = 0$, the first term equals $-\mathbf{v}^\top \mathbf{D} \mathbf{v} > 0$ since \mathbf{D} is of strictly negative type. $\mathbf{1}^\top \mathbf{Z} \mathbf{1} \geq n$ since $Z_{ii} = 1$ and $Z_{ij} \geq 0$. Therefore, $a^2 \mathbf{1}^\top \mathbf{Z} \mathbf{1} \geq na^2 \geq 0$. Thus, when the cross-term $2a\mathbf{v}^\top \mathbf{Z} \mathbf{1}$ is non-negative, $\mathbf{x}^\top \mathbf{Z} \mathbf{x} > 0$ as desired. When $\mathbf{1}$ is an eigenvalue of \mathbf{Z} , we can substitute $\mathbf{Z} \mathbf{1} = \lambda \mathbf{1}$ in the cross-term to get $2a\lambda \mathbf{v}^\top \mathbf{1} = 0$. This concludes the proof. \square

We emphasise that this is a one-way implication and not an equivalence. The Rutor glacier analysis shows that the conditions are not necessary.

Appendix C: Runtime compared to OT

The comparison in the main paper also holds for $\alpha = 3$ (Fig. S1).

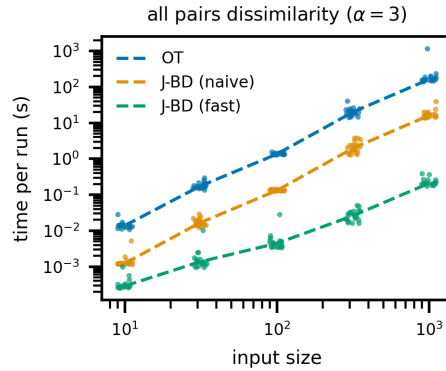


FIG. S1. **Comparing runtime with OT for $\alpha = 3$.** The runtime in seconds as a function of the number of input distributions for the all-pairs dissimilarity task. The points mark the results from 20 runs each for OT (blue), J-BD (naive) (orange), and J-BD (fast) (green). The lines connect the medians. Note the log scale on both axes.

Appendix D: The geography of occupations in England and Wales

1. Tradable occupations

Our analysis focuses on ‘tradable’ occupations that likely create outputs that are not solely for the local population. Our method relying on correlations yields a similar ranking of tradability as locational Gini (Fig. S2). We identify 41 tradable occupations (Table S1).

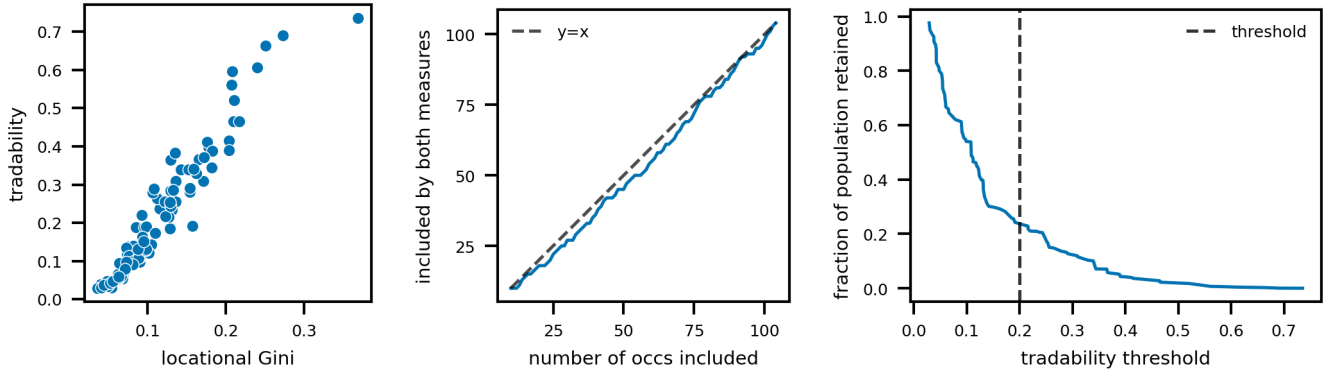


FIG. S2. **Identifying tradable occupations.** (Left) Tradability vs locational Gini index. (Middle) Ranking by these indices, we plot the number of occupations that would have been included by both measures against the number of occupations included. (Right) The fraction of workforce retained as a function of the tradability threshold. We pick a threshold of 0.2, which includes occupations employing 24% of the workforce.

2. Similarity matrices

In the main paper, we analysed three similarity matrices, modelling no similarity, skills similarity, and co-location similarity. Here, we also include a fourth: hierarchy similarity, which is defined using the occupation classification taxonomy. The code for constructing them is available on our GitHub repository. See Fig. S3.

a. Skills similarity We use the ONET mapping of occupations to skills, which assigns an importance score between 1 and 5 to each of the 35 skills. Each of our 3 digit SOC2020 occupations are matched to multiple ONET occupations by the NFER’s mapping. We assign a skill vector to our occupations by taking the mean of the matched ONET occupations’. Of the 394 ONET occupations in the matching, 20 do not have skills data. This only affects 12 of our occupations, each of which have multiple other ONET occupations to estimate skills from (see software release for details).

The skills are Reading Comprehension, Active Listening, Writing, Speaking, Mathematics, Science, Critical Thinking, Active Learning, Learning Strategies, Monitoring, Social Perceptiveness, Coordination, Persuasion, Negotiation, Instructing, Service Orientation, Complex Problem Solving, Operations Analysis, Technology Design, Equipment Selection, Installation, Programming, Operations Monitoring, Operation and Control, Equipment Maintenance, Troubleshooting, Repairing, Quality Control Analysis, Judgment and Decision Making, Systems Analysis, Systems Evaluation, Time Management, Management of Financial Resources, Management of Material Resources, and Management

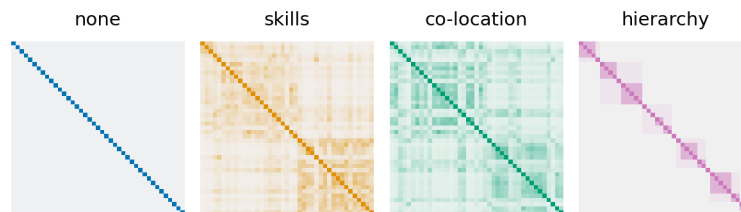


FIG. S3. **Similarity matrices.**

Code	Occupation	Population (%)
111	Chief Executives and Senior Officials	1.9
113	Functional Managers and Directors	14.6
114	Directors in Logistics, Warehousing and Transport	0.2
116	Senior Officers in Protective Services	0.7
121	Managers and Proprietors in Agriculture Related Services	0.8
211	Natural and Social Science Professionals	1.5
214	Web and Multimedia Design Professionals	1.4
215	Conservation and Environment Professionals	0.6
216	Research and Development (R&D) and Other Research Professionals	1.3
224	Veterinarians	0.3
241	Legal Professionals	3.4
242	Finance Professionals	5.7
243	Business, Research and Administrative Professionals	5.1
247	Librarians and Related Professionals	0.3
249	Media Professionals	2.2
312	CAD, Drawing and Architectural Technicians	0.9
324	Veterinary nurses	0.3
331	Protective Service Occupations	5.2
341	Artistic, Literary and Media Occupations	5.1
342	Design Occupations	1.0
351	Transport Associate Professionals	0.4
353	Finance Associate Professionals	2.8
411	Administrative Occupations: Government and Related Organisations	4.1
511	Agricultural and Related Trades	4.4
521	Metal Forming, Welding and Related Trades	1.2
522	Metal Machining, Fitting and Instrument Making Trades	3.8
523	Vehicle Trades	3.3
525	Skilled Metal, Electrical and Electronic Trades Supervisors	0.6
541	Textiles and Garments Trades	0.6
542	Printing Trades	0.4
612	Animal Care and Control Services	1.2
811	Process Operatives	3.7
812	Metal Working Machine Operatives	0.7
813	Plant and Machine Operatives	1.3
814	Assemblers and Routine Operatives	2.8
816	Production, Factory and Assembly Supervisors	0.9
822	Mobile Machine Drivers and Operatives	1.9
823	Other Drivers and Transport Operatives	1.1
911	Elementary Agricultural Occupations	0.8
913	Elementary Process Plant Occupations	3.4
925	Elementary Storage Occupations	8.2

TABLE S1. **Tradable occupations in England and Wales.** The 41 occupations in our analysis along with their share of the population. The occupations are classified by SOC 2020.

of Personnel Resources.

b. Hierarchy similarity Occupations have a similarity of 0.5 if they are identical at 2 digit level, 0.1 if they are identical at 1 digit level, and 0 otherwise.

3. Diversity and representativeness

In the main paper, we reported values for the correlations of rankings by entropy and divergence from the population's occupation composition for $\alpha = 2$. The differences are also apparent for other values of α (Tables S2 and S3).

$\alpha = 2$	none	skills	co-location	hierarchy
none	1.000	0.631	0.677	0.811
skills	0.631	1.000	0.536	0.640
co-location	0.677	0.536	1.000	0.782
hierarchy	0.811	0.640	0.782	1.000
$\alpha = 3$	none	skills	co-location	hierarchy
none	1.000	0.585	0.642	0.807
skills	0.585	1.000	0.523	0.629
co-location	0.642	0.523	1.000	0.764
hierarchy	0.807	0.629	0.764	1.000
$\alpha = 4$	none	skills	co-location	hierarchy
none	1.000	0.566	0.634	0.812
skills	0.566	1.000	0.510	0.627
co-location	0.634	0.510	1.000	0.754
hierarchy	0.812	0.627	0.754	1.000

TABLE S2. Kendall's τ between rankings of LAs by diversity.

$\alpha = 2$	none	skills	co-location	hierarchy
none	1.000	0.787	0.799	0.888
skills	0.787	1.000	0.899	0.871
co-location	0.799	0.899	1.000	0.882
hierarchy	0.888	0.871	0.882	1.000
$\alpha = 3$	none	skills	co-location	hierarchy
none	1.000	0.759	0.727	0.848
skills	0.759	1.000	0.904	0.872
co-location	0.727	0.904	1.000	0.847
hierarchy	0.848	0.872	0.847	1.000
$\alpha = 4$	none	skills	co-location	hierarchy
none	1.000	0.741	0.695	0.838
skills	0.741	1.000	0.883	0.847
co-location	0.695	0.883	1.000	0.816
hierarchy	0.838	0.847	0.816	1.000

TABLE S3. Kendall's τ between rankings of LAs by representativeness.

4. Regionalisation

We plot the maps depicting the optimal clusters for $k = 2$ and 3 in Figs S4 and S5 respectively.

Appendix E: β -diversity of vegetation in the Rutor Glacier

The results in the main paper are qualitatively robust to $\alpha = 3$ and 4 (Fig. S6).

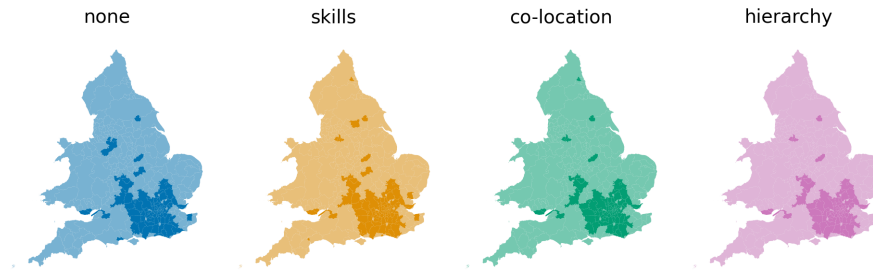


FIG. S4. **Geography of the optimal two-way partition by occupational composition.** The partitions capture the concentration of white collar occupations in the south.

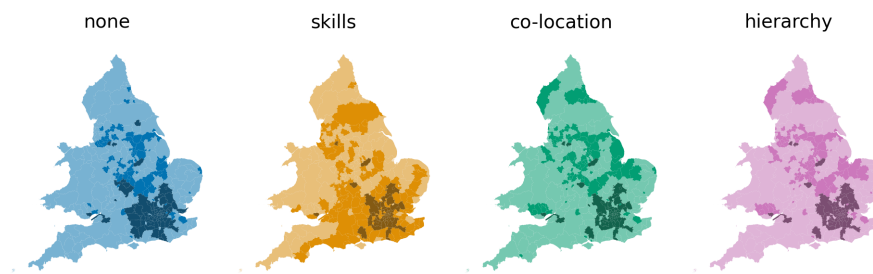


FIG. S5. **Geography of the optimal three-way partition by occupational composition.** These partitions are discussed in the main paper.

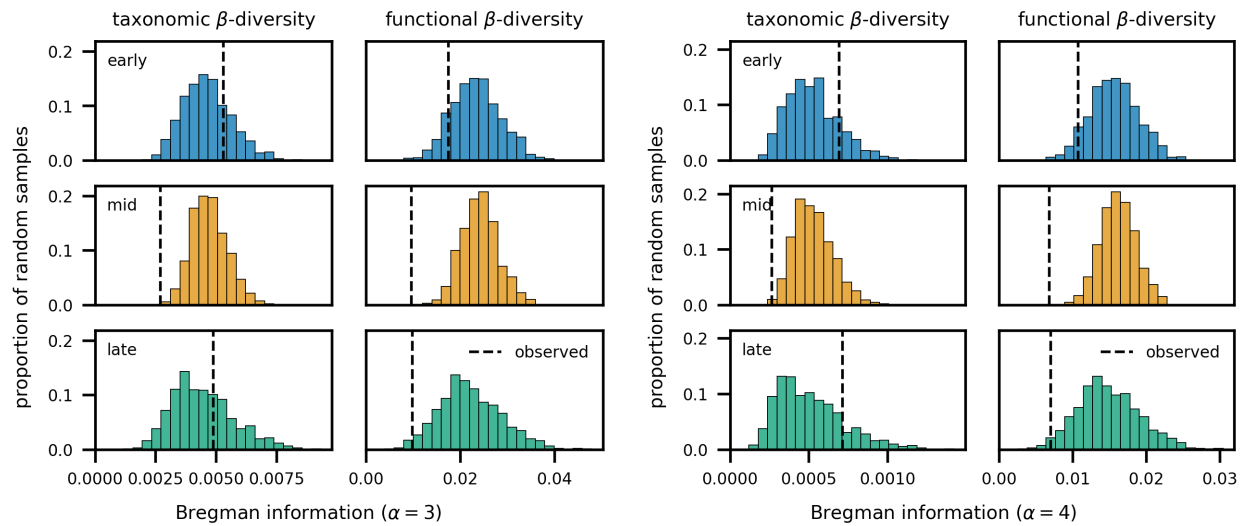


FIG. S6. **β -diversity of the successional stages of the Rutor glacier.** These plots show the results reported in Fig. 5 for $\alpha = 3$ and 4.